Influence of poly(3,4-ethylenedioxythiophene)-poly(styrenesulfonate) in polymer LEDs

P. J. Brewer,[1,*] J. Huang,[2] P. A. Lane,[3] A. J. deMello,[1] D. D. C. Bradley,[2] and J. C. deMello[1,†]
[1]*Department of Chemistry, Imperial College London, London, SW7 2AZ UK*
[2]*Blackett Laboratory, Imperial College London, London SW7 2BZ UK*
[3]*Naval Research Laboratory, Washington, D.C., USA*
(Received 11 May 2006; published 11 September 2006)

We investigate the influence of poly(3,4-ethylenedioxythiophene)-poly(styrenesulfonate) (PEDOT:PSS) on the optoelectronic properties of polymer light-emitting diodes containing poly(9,9-dioctylfluorene) (PFO). Electromodulation and *IV* luminance measurements are reported for a series of devices with bare indium tin oxide (ITO) or PEDOT:PSS-coated ITO anodes and Ba or Al cathodes. The ITO/PFO/Al, ITO/PFO/Ba, and ITO/PEDOT:PSS/PFO/Al devices all exhibit conventional field-induced electromodulation behavior, in both forward and reverse bias, consistent with the Stark effect (SE). The ITO/PEDOT:PSS/PFO/Ba devices by contrast exhibit conventional behavior only for applied biases below the flat-band voltage; at higher biases, the field-induced SE features vanish and are replaced by anomalous charge-induced electromodulation features. This anomalous behavior is observed only when PEDOT:PSS is used in conjunction with a strongly electron-injecting cathode such as Ba, and is attributed to the presence of trapped electrons at the PEDOT:PSS-emitter interface, which screen the electric field from the bulk of the device. The enhanced field at the interface increases the rate of field-assisted hole injection into the highest occupied molecular orbital (HOMO) of the PFO, resulting in lower drive voltages and increased electroluminescence efficiencies.

DOI: 10.1103/PhysRevB.74.115202 PACS number(s): 78.20.Jq

INTRODUCTION

Semiconducting polymers are of scientific and commercial interest owing to their applications in optoelectronic devices such as light-emitting diodes, solar cells, and thin-film transistors.[1] There has been significant progress in the development of polymer devices in recent years with, for example, displays based on polymer light-emitting diodes (LEDs) now entering the market place as viable contenders to LCDs. To some extent, however, attempts to optimize the efficiencies and performance of polymer LEDs have been hindered by the relative absence of detailed models describing device operation. The fundamental processes governing device characteristics are the subject of debate and there is considerable interest in experimental measurements that provide insight into device operation.

In previous studies, we used electromodulation (EM) spectroscopy to investigate the internal electric-field strength in operational polymer light-emitting diodes containing poly(3,4-ethylenedioxythiophene)-poly(styrenesulfonate) (PEDOT:PSS).[2–5] These measurements indicated that, for many polymer LEDs under light emission conditions, screening effects by injected charge carriers lead to near-complete cancellation of the internal field. In the absence of a sizeable bulk field—and hence drift current—carrier transport is mediated primarily by diffusion in a manner similar to light-emitting electrochemical cells.[6] More recently, by fabricating two device types in which the cathode material was selected to provide either efficient (Ba) or inefficient (Al) electron injection, we were able to show that injected electrons trapped close to the anode are responsible for the field redistribution.[5] In short, only the Ba devices exhibited screening effects, indicating that efficient electron injection is a necessary condition to observe screening. The trapped electrons close to the hole-injecting contact cause the potential to drop preferentially at this location, thereby reducing the magnitude of the bulk field. The high-field strength at the PEDOT:PSS-polyfluorene interface results in efficient hole injection even when sizeable energy offsets exist between the Fermi level of the PEDOT:PSS and the highest occupied molecular orbital (HOMO) of the active layer. These conclusions are in agreement with independent studies by Murata *et al.*,[7] Van Woudenbergh *et al.*,[8] and Poplavskyy *et al.*[9] who, based on analysis of current-voltage characteristics and other measurements, also found evidence for electron accumulation close to the hole-injecting contact.

In previous papers we noted that we had only observed anomalous electromodulation effects in devices containing PEDOT:PSS at the hole injecting contact.[2–5] In this paper, we investigate this issue in more detail by comparing the electromodulation response of a series of devices, fabricated with and without a PEDOT:PSS hole injection layer. Since PEDOT:PSS is found in practically all "state-of-the-art" polymer LEDs, its influence on device operation is an issue of considerable pertinence, and electromodulation studies offer a potentially powerful means of investigating this issue.

EXPERIMENTAL OVERVIEW

A series of devices with and without PEDOT:PSS were fabricated using poly(9,9-dioctylfluorene) (PFO) as the active layer. The PEDOT:PSS-free devices were fabricated by spin-coating 130-nm layers of PFO onto indium tin oxide (ITO) coated glass from a 15-mg/ml solution of PFO in chloroform. The deposited films were then annealed in a dry nitrogen atmosphere at 60 °C for 2 h prior to thermal deposition of a Ba or Al cathode. The choice of cathode material determines the efficiency of electron injection, with Ba providing good injection and Al providing poor injection. The PEDOT:PSS devices were fabricated in the same manner, but

an 80-nm layer of as-received PEDOT:PSS (Baytron P formulation from H. C. Starck GmbH) was spin coated onto the ITO anode (and subsequently annealed in a dry nitrogen atmosphere at 200 °C for 8 min to drive off residual water) prior to deposition of the PFO layer. The completed devices were encapsulated in a nitrogen atmosphere glovebox. In the following text and the associated figures, the various devices are denoted by the labels (a), (b), (c), and (d), which correspond, respectively, to the structures ITO/PFO/Al, ITO/PFO/Ba, ITO/PEDOT:PSS/PFO/Al, and ITO/PEDOT:PSS/PFO/Ba. The corresponding current-voltage characteristics were measured using a Keithley 2410 Source Measure Unit and the luminance was measured with a calibrated TOPCON Luminance Meter.

EM spectroscopy has been widely used to investigate internal electric fields in organic devices.[10–16] In a typical EM measurement, a combined ac and dc bias $V=V_{\mathrm{dc}}+V_{\mathrm{ac}}\sin(\omega t)$ is applied to the device and changes in the transmission of a probe beam are monitored using phase sensitive lock-in detection. If the origin of the EM signal is electroabsorption (i.e., the Stark effect), the fractional change in transmission is proportional to the third-order dc Kerr nonlinear susceptibility and the square of the electric field. (Please note, the terms electroabsorption (EA) and Stark effect (SE) are used interchangeably in this paper.) The differential transmission is therefore modulated at both the first- and second-harmonic frequencies in accordance with Eqs. (1a) and (1b),

$$I_{1\omega}=\left.\frac{\Delta T}{T}\right|_{1\omega}\propto 2\,\mathrm{Im}\,\chi^{3}(\lambda)E_{dc}E_{ac}\sin(\omega t), \tag{1a}$$

$$I_{2\omega}=\left.\frac{\Delta T}{T}\right|_{2\omega}\propto \tfrac{1}{2}\mathrm{Im}\,\chi^{3}(\lambda)E_{ac}^{2}\cos(2\omega t). \tag{1b}$$

Under conditions of low carrier injection, the bulk field E_{dc} is related to the dc component of the applied voltage V_{dc} by $E_{\mathrm{dc}}=(V_{\mathrm{dc}}-V_{\mathrm{bi}})/d$ where V_{bi} is the built-in potential, and d is the width of the device. I_{ω} therefore varies linearly with V_{dc} (passing through zero at $V=V_{\mathrm{bi}}$), and $I_{2\omega}$ is independent of V_{dc}; any deviations from this behavior indicate nonuniform internal fields arising from the presence of substantial charge in the device (or, in the case of multilayer devices, contributions from different layers that have distinct spectral characteristics).

The measurement of electromodulation spectra in operational LEDs is complicated by the presence of strong modulated electroluminescence (EL) that is typically several orders of magnitude larger than the EM signal. All measurements reported here were therefore obtained using the double modulation approach of Pires *et al.*,[17] which permits the measurement of EM signals as small as one part in 10^{7} even for highly emissive operational devices. In this approach, the applied bias is modulated at a frequency ω_{osc} and the probe beam is modulated with an optical chopper at a lower frequency ω_{probe}. Two lock-in amplifiers are used, the first acting as a (low time-constant) prefilter tuned to ω_{osc} and the second locking into the ω_{probe} frequency component of the prefiltered signal. This procedure is slightly different from the double modulation technique we used in previous papers, in which $\omega_{\mathrm{probe}}\gg\omega_{\mathrm{osc}}$ and the first and second lock-in amplifiers were locked into ω_{probe} and ω_{osc}, respectively. This latter arrangement is convenient because the dc component of the filtered signal from the first lock-in provides a direct measurement of the transmitted signal T, obviating the need for a separate measurement. However, it has the disadvantage that ω_{osc} must be significantly lower than ω_{probe}, which in practical terms limits the bias modulation frequency to around 1 kHz when a mechanical chopper wheel is used for optical modulation. The alternate arrangement used here necessitates a separate measurement of the transmission T but does not impose any upper limit on ω_{probe}.

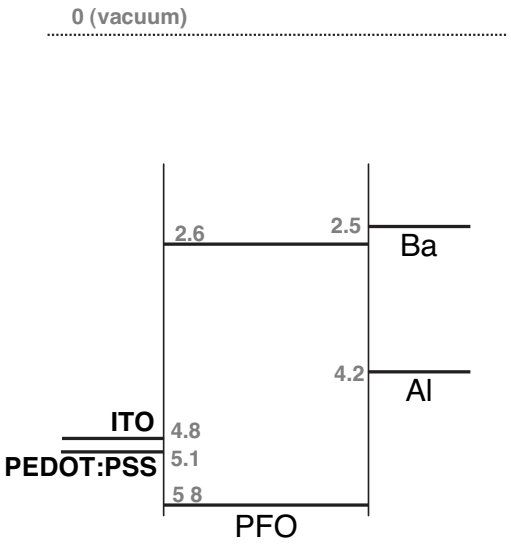

FIG. 1. A schematic energy-level diagram for the device materials used in this work.

RESULTS

Figure 1 shows approximate values for the work functions of ITO, PEDOT:PSS, Ba, and Al and for the HOMO and lowest unoccupied molecular orbital (LUMO) energies of PFO. The approximate barrier height for hole injection into the HOMO level of PFO is 1.0±0.2 eV for ITO and 0.7±0.2 eV for PEDOT:PSS, both of which are relatively large values that would ordinarily be expected to inhibit hole injection substantially. The approximate barrier height for electron injection from Al into the LUMO level of PFO is 1.6±0.2 eV—a very large value that would result in minimal electron injection under ordinary circumstances. In the case of Ba, the Fermi level lies approximately 0.1 eV above the LUMO level of PFO so Ohmic electron injection is expected. Hence on the basis of simple energy considerations, for both ITO- and ITO/PEDOT:PSS-based devices, we would expect devices with Al cathodes to show low currents (due to poor electron and hole injection) and devices with Ba cathodes to show high currents (due to good electron injection) but low EL efficiencies (due to poor hole injection).

The *IV* luminance characteristics of devices (a) (ITO/PFO/Al), (b) (ITO/PFO/Ba), (c) (ITO/PEDOT:PSS/PFO/Al)

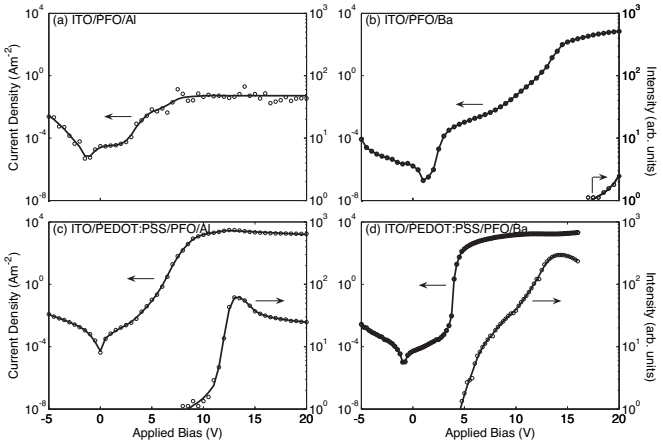

FIG. 2. *IV* luminance measurements for the (a) ITO/PFO/Al, (b) ITO/PFO/Ba, (c) ITO/PEDOT:PSS/PFO/Al, and (d) ITO/PEDOT:PSS/PFO/Ba devices. Device (d) shows a sharp threshold for current injection at 3 V that is not observed in the other devices. This sharp threshold is observed only in the presence of a PEDOT:PSS anode and a low work-function cathode such as Ba or Ca.

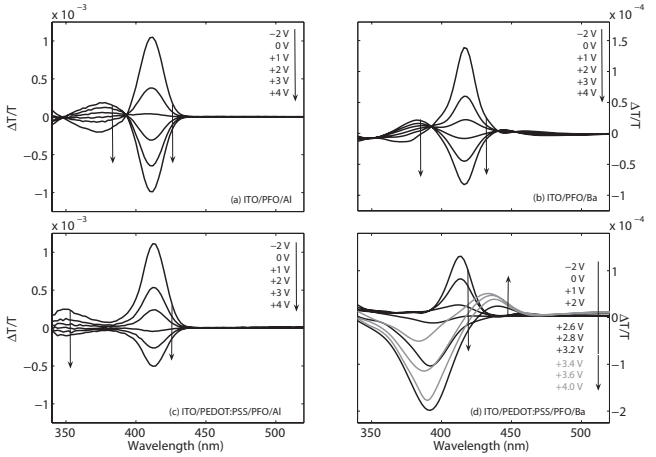

FIG. 3. The 6-kHz first-harmonic electromodulation spectra of the (a) ITO/PFO/Al, (b) ITO/PFO/Ba, (c) ITO/PEDOT:PSS/PFO/Al, and (d) ITO/PEDOT:PSS/PFO/Ba devices at a variety of dc biases. The EM spectra of devices (a), (b), and (c) scale approximately linearly with the dc bias but otherwise do not change significantly in shape, consistent with electroabsorption. The reverse bias EM spectra of device (d) are similar to those of the other devices but, in forward bias, the spectra change completely and the EM features are replaced by new absorption features due to injected charge. These anomalous forward bias features are observed only in the presence of a PEDOT:PSS anode and a low work-function cathode such as Ba or Ca.

and (d) (ITO/PEDOT:PSS/PFO/Ba) are shown in Figs. 2(a)–2(d), respectively. A delay of 10 s between initial application of the step voltage and each measurement was employed to allow reasonable time for steady state to be achieved. The ITO/PFO/Al device was by far the most resistive of the four devices, consistent with the large barrier heights for both electron and hole injection. The ITO/PFO/Ba device exhibited much higher current densities than the ITO/PFO/Al device due to the greatly improved electron injection, and weak light emission was detectable above 17 V. The ITO/PEDOT:PSS/PFO/Al device also exhibited much higher current densities than the ITO/PFO/Al device, with detectable light emission above 8 V. Interestingly, the current density and EL intensity of the ITO/PEDOT:PSS/PFO/Al device were both substantially higher than for the ITO/PFO/Ba device. This is somewhat surprising since energy-level considerations suggest the Ba/PFO interface should form an Ohmic contact for electron injection whereas a 0.7-eV barrier to hole injection should exist at the PEDOT:PSS/PFO interface, significantly impeding hole injection. Time-of-flight measurements, however, indicate that hole transport is much better than electron transport in PFO due to shallow trapping of electrons in the polymer bulk.[18] In the present devices, it therefore appears that the injection-limited hole current in the ITO/PEDOT:PSS/PFO/Al device wins out over the bulk-limited electron current in the ITO/PFO/Ba device. The *IV* luminance characteristics of the ITO/PEDOT:PSS/PFO/Ba device are shown in Fig. 2(d), and stand out clearly from the other devices. There is an extremely sharp current threshold at 3 V that coincides closely with the onset of measurable light emission. The intensity of this emission is much stronger than for the ITO/PFO/Ba and ITO/PEDOT:PSS/PFO/Al devices, even though the current densities are comparable in the range 10–20 V, indicating significantly enhanced EL efficiencies in the ITO/PEDOT:PSS/PFO/Ba device. This sharp threshold, which results in greatly improved power efficiencies due to the lower operating voltage and higher EL quantum efficiency, is a common feature of devices containing both PEDOT:PSS and a low work function cathode.

Further insight into the anomalous behavior of the ITO/PEDOT:PSS/PFO/Ba device, and in particular the cause of the sharp threshold, can be obtained from EM spectroscopy. Figure 3 shows for a variety of applied biases the first harmonic electromodulation spectra for the four device structures described above. The EM response of the ITO/PFO/Al and ITO/PFO/Ba devices are shown in Figs. 3(a) and 3(b). The devices have similar oscillatory electromodulation features with common peaks at ~375 and 415 nm and common nodes at 350 and 395 nm (although in the case of the ITO/PFO/Al device the profile of the 350-nm feature is considerably more symmetrical). In addition, the ITO/PFO/Ba device shows two additional weak subband-gap features centered at 446 and 470 nm (with symmetric and asymmetric profiles, respectively). The EM response of the ITO/PEDOT:PSS/PFO/Al device [Fig. 3(c)] is qualitatively similar to the PEDOT:PSS-free devices, showing the same dominant feature at 415 nm but lacking the nodes at 350 and 395 nm. The EM response below 390 nm is dominated at all biases by a single broad feature, centered at around 350 nm. The response beyond 440 nm is devoid of the low-energy features observed in the ITO/PFO/Ba device. For each of the devices (a), (b), and (c), the magnitude of the EM features vary approximately linearly with the applied dc bias, and the normalized profiles of the individual spectra are largely independent of dc bias. The EM response of the ITO/PEDOT:PSS/PFO/Ba device, however, again stands out as strikingly different [see Fig. 2(d)]. The reverse bias EM response is

comparable to that of the ITO/PEDOT:PSS/PFO/Al, with the same dominant feature at 415 nm and the same broad high-energy feature centered at 350 nm but the spectra change radically in forward bias. In particular, the dominant electroabsorption feature at 415 nm disappears in forward bias, and is replaced by a broad electromodulation feature with a peak wavelength of 390 nm. This feature increases rapidly with applied bias until 3.2 V, above which it starts to diminish and a new 440-nm subgap feature starts to appear.

The behavior of the ITO/PEDOT:PSS/PFO/Ba device is complex and we do not yet have a complete understanding of the electromodulation response. However, it is possible to draw some broad conclusions from the data. The similarity of the reverse bias responses of the ITO/PEDOT:PSS/PFO/Ba and ITO/PEDOT:PSS/PFO/Al devices (and the clear differences from the PEDOT:PSS-free devices) suggest that the broad 350-nm feature is directly attributable to the presence of PEDOT:PSS. Moreover, since the conductivity of the PEDOT:PSS is high compared to the (undoped) PFO, the 350-nm feature is unlikely to arise from the electromodulation response of the bulk PEDOT:PSS (since the electric potential will be dropped preferentially across the resistive PFO layer). The 350-nm feature is therefore attributable either to a thin surface region in the PEDOT:PSS close to the PEDOT:PSS/PFO interface or to chemical modification of the PFO at the interface by the PEDOT:PSS. The surface of PEDOT:PSS is known to contain an excess of PSS, which is both insulating and acidic,[19] so both explanations are feasible. The electromodulation response of the ITO/PEDOT:PSS/PFO/Al device varies linearly with dc bias over the full bias range, consistent with the Stark effect. In the case of the ITO/PEDOT:PSS/PFO/Ba device, however, the spectrum changes dramatically in forward bias, under which conditions carrier injection is substantial, and it is therefore reasonable to attribute this behavior to the influence of the injected carriers. This inference is supported by recent work on LUMATION green 1300 Series LEPs,[20] in which we were able to suppress the anomalous forward-bias features and restore the conventional electroabsorption response by reducing the operating temperature of the devices in order to lower the circulating current: when operating at 100 K, the anomalous charge-induced features did not appear until applied dc biases of 5.5 V compared with 1.2 V at room temperature.[21]

The suppression of EA features in forward bias is an interesting effect that we have seen in a wide variety of devices containing PEDOT:PSS and which we have previously attributed to screening of the internal field by injected charges.[2–5] In order to screen the bulk semiconductor from the external field, the injected charges must accumulate at the counter electrode with electrons building up at the anode and/or holes building up at the cathode. The loss of EA signal in the ITO/PEDOT:PSS/PFO/Ba device but not in the weakly electron injecting ITO/PEDOT:PSS/PFO/Al device indicates that trapped electrons are responsible for the screening effect in agreement with previous measurements we have reported for LEDs containing blends of PFO and poly(9,9-dioctylfluorene-alt-benzothiadiazole) (5BTF8).[5] Moreover, the absence of comparable effects in the ITO/PFO/Ba device indicates that the presence of *both* PEDOT:PSS *and* Ba (or comparable low work-function metal) is required for significant field redistribution to occur.

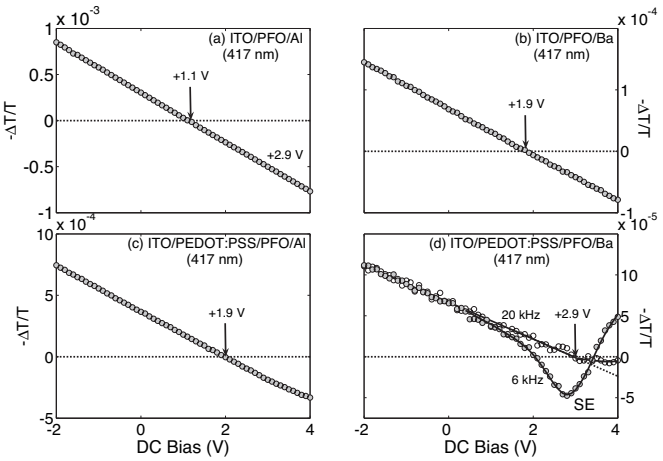

FIG. 4. The dc bias dependence of the 6-kHz 417-nm first-harmonic electromodulation response of the (a) ITO/PFO/Al, (b) ITO/PFO/Ba, (c) ITO/PEDOT:PSS/PFO/Al, and (d) ITO/PEDOT:PSS/PFO/Ba devices. The 417-nm signals vary linearly with dc bias for devices (a)–(c), consistent with electroabsorption. In the case of device (d), the signal varies linearly with dc bias in reverse bias but deviates sharply from linearity in forward bias due to charge-induced modulation. The contribution from charge-induced modulation is eliminated at high modulation frequencies (20 kHz, open circles), leaving an electromodulation signal that is due primarily to the Stark effect. This SE-only signal falls linearly to zero at 2.9 V (which is the approximate threshold for current injection), and remains at zero for higher biases.

In Fig. 4 we show the dc bias dependence of the first-harmonic EM response for the four devices, measured at the 417-nm EA peak using a 6-kHz, 0.35-V rms ac bias. The response of the ITO/PFO/Al, ITO/PFO/Ba, and ITO/PEDOT:PSS/PFO/Al devices all vary linearly with the dc bias in agreement with Eq. (1a), passing through zero at 1.1 and 1.9 V, respectively. The 6-kHz EM response of the ITO/PEDOT:PSS/PFO/Ba device, denoted by the filled circles in Fig. 4(d), however, is again strikingly different. The signal varies linearly with dc bias until ~0.8 V, at which point it deviates significantly in the direction of negative $\Delta T/T$ as charge-induced absorption effects become important. The emergence of the charge-induced features obscures the behavior of the EA peak at 417 nm making it difficult to draw conclusions about the internal field. In Refs. 3 and 4 we reported that the charge-induced features show a strong reduction in intensity with increasing modulation frequency whereas the EA signal is frequency independent due to the near-instantaneous nature of the Stark effect. The dc bias dependence of the EA signal is therefore best measured at high frequencies where contamination from charge-induced contributions is minimal. As discussed above, the experimental configuration used in previous work[4,5] placed a practical upper limit of 1 kHz on the ac bias frequency due to the ceiling imposed by the optical chop frequency. In this work, however, using the modified configuration described above, we were able to perform measurements up to 20 kHz (with the upper frequency now being determined by the bandwidth

of our photodetector). At this higher frequency, the EM response of the ITO/PEDOT:PSS/PFO/Ba device is found to decrease linearly with applied bias until the zero crossing is reached at 2.9 V in a similar manner to the EM response of the other devices. However, the signal does not subsequently rise in magnitude as would be expected for the formation of a forward biased electric field in the device. Instead, it remains at zero indicating full neutralization of the internal field due to the trapped electrons (see Ref. 4 for a detailed discussion of the screening effect). This is consistent with previous low-frequency (<1 kHz) measurements we reported on a commercial red-emitting polyfluorene-based copolymer in which spectral regions could be identified where the measured EM signal was due entirely to the Stark effect, with negligible contamination from charge-induced modulation.[22]

The anomalous behavior of the ITO/PEDOT:PSS/PFO/Ba device in Figs. 3 and 4 provides valuable insight into the improved charge injection and EL efficiencies seen in Fig. 2. Above the turn-on voltage, the Ohmically injected electrons accumulate in trap sites close to the PEDOT:PSS/PFO interface, which causes the potential to be dropped preferentially in this location and leaves the bulk semiconductor screened from the applied electric field. The enhanced electric field at the PEDOT:PSS/PFO interface increases the rate of field-dependent hole injection, resulting in a sizeable hole current even at low drive voltages despite the substantial barrier to hole injection. The enhanced hole injection improves the balance of electron and hole injection currents in the device resulting in greatly improved EL efficiencies. A detailed description of this mechanism can be found in Ref. 4. Importantly, the measurements outlined here add to our previous work by providing direct evidence that the electron traps are due to the presence of PEDOT:PSS. The role of PEDOT:PSS in electron trapping has also been postulated by Poplavskyy *et al.*[9] and Van Woudenbergh *et al.*[23] The latter authors found that polymer light-emitting diodes (LEDs) containing poly(9,9-dioctylfluorene) (PFO) and a PEDOT:PSS hole injection layer exhibited strongly enhanced hole currents compared to devices with uncoated Ag and ITO anodes. In practical terms, devices that incorporate a PEDOT:PSS hole injection layer represent the present state of the art in terms of polymer LED power efficiencies and operational lifetimes. However, the chemical and physical nature of the trap sites that are responsible for the improved performance are still unclear, and future studies will seek to shed light on this issue, with a view to developing new materials with improved performance. The ultimate objective of such work would be the creation of a new generation of polymer LEDs, in which electron and hole traps are deliberately introduced close to the anode and cathode, respectively, to improve electron and hole injection simultaneously.

CONCLUSION

In conclusion we have fabricated ITO/PFO/metal and ITO/PEDOT:PSS/PFO/metal devices, where the top metallic electrode was chosen as either Ba or Al to provide respectively efficient or inefficient electron injection. The ITO/PFO/Al, ITO/PFO/Ba, and ITO/PEDOT:PSS/PFO/Al devices had similar oscillatory first-harmonic EM spectra that scaled linearly with dc bias, consistent with conventional field-induced electroabsorption. The ITO/PEDOT:PSS/PFO/Ba devices by contrast showed conventional SE behavior only at low applied biases; above turn-on, the SE features vanished due to screening of the internal field and were replaced by charge-induced absorption features. The occurrence of these anomalous features only when both PEDOT:PSS and a low work-function cathode are present in the device indicates that the screening is due to trapped electrons at the PEDOT:PSS/PFO interface. The high field strength at the anode due to the trapped electrons is beneficial for device operation since it increases the rate of (field-dependent) hole injection, resulting in balanced injection of electrons and holes and higher device efficiencies. PEDOT:PSS is found in practically all state-of-the-art polymer LEDs, and we consider that its widespread utility is a direct consequence of the anomalous behavior outlined in this and previous papers.

ACKNOWLEDGMENTS

We would like to thank the Dow Chemical Company for providing the polymers used in this study. We also thank The Sumation Co. Ltd. for permission to publish this work: Sumation now holds the rights to the Lumation family of polyfluorenes and should be contacted for any future inquiries thereon. We additionally thank the UK Engineering and Physical Sciences Research Council for financial support (Grant No. GR/S96791/01 and Grant No. GR/S81650/01).

*Present address: National Physical Laboratory, Teddington, Middlesex, TW11 0LW UK.

†Author to whom correspondence should be addressed. Email address: j.demello@imperial.ac.uk

[1] R. H. Friend, R. W. Gymer, A. B. Holmes, J. H. Burroughes, R. N. Marks, C. Taliani, D. D. C. Bradley, D. A. D. Santos, J. L. Brédas, M. Lögdlund, and W. R. Salaneck, Nature (London) **397**, 121 (1999).

[2] P. A. Lane, J. C. deMello, R. B. Fletcher, and M. Bernius, Appl. Phys. Lett. **83**, 3611 (2003).

[3] P. A. Lane, J. C. deMello, R. B. Fletcher, and M. I. Bernius, Proc. SPIE **5214**, 162 (2004).

[4] P. J. Brewer, P. A. Lane, A. J. deMello, D. D. C. Bradley, and J. C. deMello, Adv. Funct. Mater. **14**, 562 (2004).

[5] P. J. Brewer, P. A. Lane, J. Huang, A. J. deMello, D. D. C. Bradley, and J. C. deMello, Phys. Rev. B **71**, 205209 (2005).

[6] J. C. deMello, N. Tessler, S. C. Graham, and R. H. Friend, Phys. Rev. B **57**, 12951 (1998).

[7] K. Murata, S. Cina, and N. C. Greenham, Appl. Phys. Lett. **79**, 1193 (2001).

[8] T. V. Woudenbergh, P. W. M. Blom, and J. N. Huiberts, Appl. Phys. Lett. **82**, 985 (2003).
[9] D. Poplavskyy, J. Nelson, and D. D. C. Bradley, Appl. Phys. Lett. **83**, 707 (2003).
[10] C. Giebeler, S. A. Whitelegg, A. J. Campbell, M. Liess, S. J. Martin, P. A. Lane, D. D. C. Bradley, G. Webster, and P. L. Burn, Appl. Phys. Lett. **74**, 3714 (1999).
[11] J. C. deMello, J. J. M. Halls, S. C. Graham, N. Tessler, and R. H. Friend, Phys. Rev. Lett. **85**, 421 (2000).
[12] I. H. Campbell, T. W. Hagler, D. L. Smith, and J. P. Ferraris, Phys. Rev. Lett. **76**, 1900 (1996).
[13] T. M. Brown, R. H. Friend, I. S. Millard, D. J. Lacey, J. H. Burroughes, and F. Cacialli, Appl. Phys. Lett. **77**, 3096 (2000).
[14] P. A. Lane, J. Rostalski, C. Giebeler, S. J. Martin, D. D. C. Bradley, and D. Meissner, Sol. Energy Mater. Sol. Cells **63**, 3 (2000).
[15] S. J. Martin, G. L. B. Verschoor, M. A. Webster, and A. B. Walker, Org. Electron. **3**, 129 (2002).
[16] I. Hiromitsu, Y. Murakam, and T. Ito, J. Appl. Phys. **94**, 2434 (2003).
[17] M. P. Pires, P. L. Souza, and J. P. V. d. Weid, Braz. J. Phys. **26**, 252 (1996).
[18] A. J. Campbell, D. D. C. Bradley, T. Virgili, D. G. Lidzey, and H. Antoniadis, Appl. Phys. Lett. **79**, 3872 (2001).
[19] M. P. deJong, L. J. V. Ijzendoorn, and M. J. A. deVoigt, Appl. Phys. Lett. **77**, 2255 (2000).
[20] Trademark of The Dow Chemical Company.
[21] P. J. Brewer, P. A. Lane, A. J. deMello, D. D. C. Bradley, and J. C. deMello, J. Appl. Phys. **99**, 114502 (2006).
[22] Additional evidence to this effect was reported in Ref. 5 by decomposing the first harmonic EM spectrum into a simple linear combination of bias-independent field and charge-induced spectra.
[23] T. V. Woudenbergh, J. Wildeman, P. W. M. Blom, J. J. A. M. Bastiaansen, and B. M. W. Langeveld-Voss, Adv. Funct. Mater. **14**, 679 (2004).